

Reduction of Aerosol Absorption in Beijing since 2007 from MODIS and AERONET

A. Lyapustin^{1,2}, A. Smirnov^{3,2}, B. Holben², M. Chin², D. G. Streets⁴, Z. Lu⁴, R. Kahn², I. Slutsker^{3,2}, I. Laszlo⁵, S. Kondragunta⁵, D. Tanre⁶, O. Dubovik⁶, P. Goloub⁶, H.-B. Chen⁷, A. Sinyuk^{3,2}, Y. Wang^{1,2}, S. Korkin^{1,2}

¹University of Maryland Baltimore County, Baltimore, MD, USA (Alexei.I.Lyapustin@nasa.gov)

²NASA Goddard Space Flight Center, Greenbelt, MD, USA

³Sigma Space Corporation, Greenbelt, MD, USA

⁴Argonne National Laboratory, Argonne, IL, USA

⁵NOAA/NESDIS/STAR, Camp Springs, Maryland, USA

⁶Laboratoire d'Optique Atmospherique, CNRS Universite de Lille, Lille, France

⁷Institute of Atmospheric Physics, CAS, Beijing, China

Abstract. An analysis of the time series of MODIS-based and AERONET aerosol records over Beijing reveals two distinct periods, before and after 2007. The MODIS data from both the Terra and Aqua satellites were processed with the new Multi-Angle Implementation of Atmospheric Correction (MAIAC) algorithm. A comparison of MAIAC and AERONET AOT shows that whereas MAIAC consistently underestimated peak AOT values by 10-20% in the prior period, the bias mostly disappears after mid-2007. Independent analysis of the AERONET dataset reveals little or no change in the effective radii of the fine and coarse fractions and of the Angstrom exponent. At the same time, it shows an increasing trend in the single scattering albedo, by ~0.02 in 9 years. As MAIAC was using the same aerosol model for the entire 2000-2010 period, the decrease in AOT

bias after 2007 can be explained only by a corresponding decrease of aerosol absorption caused by a reduction in local black carbon emissions. The observed changes correlate in time with the Chinese government's broad measures to improve air quality in Beijing during preparations for the Summer Olympics of 2008.

1. Introduction

Anthropogenic aerosols play an important climate role directly, by scattering and absorbing solar radiation, and indirectly by modifying cloud properties. Due to the complexity of aerosol processes and incomplete understanding of their interactions with the climate system, large uncertainties in climate modeling remain [IPCC, 2007]. The role of aerosols can change dramatically from cooling to warming the ambient atmosphere with an increase in their absorption, which is modulated by the amount of black carbon (BC). Anthropogenic BC is generated mainly from fossil-fuel combustion and biomass burning; the first is found to be twice as efficient a warming agent as the second [Ramana *et al.*, 2010].

Space-based remote sensing has been used to study the aerosol optical thickness (AOT) of Earth's atmosphere. Currently, the global operational AOT data over land are provided by MODIS [Levy *et al.*, 2007; Hsu *et al.*, 2004], MISR [Martonchik *et al.*, 2009; Kahn *et al.*, 2010], and, in the case of absorbing aerosols, OMI [Torres *et al.*, 2007]. Available space-based remote sensing has limited ability to evaluate aerosol absorption. MISR can distinguish two-to-four categories of absorption under favorable retrieval conditions [Chen *et al.*, 2008], whereas OMI can detect aerosols that are absorbing in the UV (Dust and organic/black carbon). The MODIS Dark Target algorithm (MOD04) retrieves AOT and Fine Mode Fraction (FMF) based on a regionally prescribed scattering and absorbing properties of the fine and coarse components derived from Aerosol Robotic Network of Sun photometer (AERONET) [Holben *et al.*, 1998] data.

Beijing is a growing megacity with a population in 2007 of over 17 million people. The very high level of air pollution in Beijing has multiple consequences, including reduced visibility and human health impacts [e.g., *Lei et al.*, 2010]. Industry, residential heating and cooking, and the transportation sectors are the main local aerosol emission sources [*Lei et al.*, 2010]. In the past decade, the Chinese government undertook measures to improve air quality, starting with the 2001 Law of Air Pollution and Control, and moving aggressively since 2005 as part of preparations for the 2008 Summer Olympics. A recession that began in the 3rd quarter of 2008 and lasted through 2009 provided a continued follow-on effect [*Lin et al.*, 2010]. Data analysis showed the effectiveness of the government measures in decreasing SO₂ during the pre-Olympic period [*Guinot et al.*, 2007]. Although a reduction of BC was reported [*Wang et al.*, 2005], its assessments remain uncertain; for example, *Guinot et al.* [2007] found that with the decrease in total carbon (TC), the BC/TC ratio in the fine aerosol mode has increased from 21% to 28% over the period 2000-2004. The present article provides new information on aerosol absorption trends in Beijing, based on an analysis of AERONET data, and MODIS data processed by the new Multi-Angle Implementation of Atmospheric Correction (MAIAC) algorithm [*Lyapustin et al.*, 2010].

2. Methods and Results

MAIAC is a new algorithm developed for MODIS, which retrieves AOT and FMF over land simultaneously with surface bidirectional reflectance parameters derived from time series analysis and image-based processing. Retrievals are performed at 1 km resolution. Following the MOD04 algorithm, models for the fine and coarse aerosol fractions are specified regionally. A comparison between MAIAC and MOD04 shows that these algorithms have generally similar accuracy over vegetated or relatively dark surfaces, and that MAIAC improves accuracy over brighter surfaces [*Lyapustin et al.*, 2010], which include most urban areas.

In this work, we consider MAIAC aerosol retrievals over Beijing (116.381°E, 39.977°N) using 50×50 km² subsets from MODIS centered on selected AERONET sites. The subsets are provided by the MODIS Operational Adaptive Processing System (MODAPS) for both the Terra and Aqua satellites. A comparison with AERONET was performed, following the MODIS validation strategy [Ichoku *et al.*, 2002]: a) The AERONET level 2 measurements are averaged over ±30 min intervals centered on overpass time. A comparison is considered valid if there are at least two measurements within the 1-hour interval. b) MAIAC data are discarded if cloud fraction in the averaging area exceeds 20% or if snow is detected.

The 1 km MAIAC AOT data show high aerosol spatial variability in the Beijing area. To account for this factor, two averaging window sizes, 10 and 20 km, were compared (50 km windows are used in MOD04 validation). The smaller window, which was found to improve correlation (r^2) by ~0.01-0.02 and to provide better matches with AERONET at peak AOT values, was used in this work. A similar result over urban areas was reported in the MISR validation study [Kahn *et al.*, 2010].

Figure 1 shows a time series of AERONET and MAIAC AOT at 0.47 μm for MODIS Terra (top) and Aqua (bottom). Visual inspection indicates two distinct periods for both Terra and Aqua: prior to ~March 2007 (period I), MAIAC rather consistently underestimates AOT by 10-20% at peak values. In the subsequent period (II), this bias mostly disappears. To verify this observation, separate MAIAC-AERONET AOT regression plots (not shown) were generated for periods I and II. Both Terra and Aqua show an increase in the regression slope, from 0.94 to 0.99 for Terra, and from 0.91 to 1.0 for Aqua between periods I and II, respectively, at average $r^2=0.88-0.92$. The regression slope is strongly controlled by the aerosol absorption. Increasing the imaginary part of refractive index n_i by 0.001 ($n_i=0.009$, single scattering albedo SSA=0.90) brings the regression slope to 1.02 for Terra and to 0.99 for Aqua for period I.

94 Figure 2 shows a time series for the AOT difference $\Delta = \text{AOT}_{\text{AER}} - \text{AOT}_{\text{MAIAC}}$ for MODIS Terra (left)
 95 and Aqua (right). These data represent all cases of moderate-to-high AOT selected according to the
 96 AERONET data ($\text{AOT}_{\text{AER}} > 0.4$). For MODIS Terra, we filtered out six outliers with higher
 97 difference values $\pm(0.6-0.8)$. Removing these (symmetric) outliers enhances coherence of the plot
 98 and has a negligible effect on the trend lines. Both Terra and Aqua show the reduction of MAIAC's
 99 bias with respect to AERONET by approximately 0.1 (Aqua) and 0.06 (Terra) over 9 years.
 100 Separating periods I and II, Aqua shows a smaller trend, and Terra shows no trend, during period I.
 101 In period II, both datasets show larger, and similar, negative trends. Reducing the threshold AOT_{AER}
 102 from 0.4 to 0.3 does not change the observed trends. The smaller change for Terra than for Aqua
 103 may be related to the diurnal cycle of SSA in Beijing [Garland *et al.*, 2009].
 104 MAIAC retrievals for the entire time series were performed using the same bi-lognormal size
 105 distribution with volumetric radius (R_v) and standard deviation (σ) of the fine (F) and coarse (C)
 106 fractions: $R_v^F = 0.15 + 0.05\tau$, $R_v^F < 0.25 \mu\text{m}$, $\sigma^F = 0.45 \mu\text{m}$; $R_v^C = 2.5 + 0.2\tau$, $R_v^C < 3 \mu\text{m}$, $\sigma^C = 0.6 \mu\text{m}$,
 107 where τ is aerosol optical thickness at $0.47 \mu\text{m}$. The dynamic growth of aerosol size with optical
 108 thickness reflects experimentally established hygroscopic particle growth [Meier *et al.*, 2009]. The
 109 complex refractive index used in the visible spectrum ($n_r = 1.44$; $n_i = 0.008$) gives $\text{SSA} = 0.91$ at 0.47
 110 μm for a typical summertime Angstrom parameter 1.2-1.3 [Eck *et al.*, 2010]. Since the same aerosol
 111 model was used in MAIAC processing for the entire period 2000-2010, the observed difference
 112 between periods I and II is most easily explained by a change in aerosol particle size and/or
 113 absorption over time, e.g., due to reduction in BC emissions. At large AOT values $\sim 1.5-3$ typical for
 114 Beijing, it is absorption that mainly controls sensitivity of retrieved AOT, which can be as high as
 115 10-15% in response to a small SSA change of 0.01.

Next, we analyzed the AERONET inversion products [Dubovik and King, 2000; Dubovik et al., 2002] (effective radii (R_{ef}) of the fine and coarse fractions and SSA) and Ångström parameter (b). Springtime dust events [Eck et al., 2010] were excluded, based on the condition $b < 0.6$. To ensure adequate accuracy of the inversion results, the AERONET Level 2 inversion quality criteria were used (≥ 21 azimuthal angles; solar zenith angle $\geq 50^\circ$; 5% residual error; $AOT_{0.44} > 0.4$ for SSA) [Holben et al., 2006; Dubovik et al., 2002; Smirnov et al., 2000]. We analyzed both daily and monthly averages. Both datasets give the same results. The monthly averages are plotted in Figure 3, which shows no significant change in R_{ef}^F . The coarse mode radius was found to increase less than retrieval uncertainties, from 2.2 to 2.3 μm , which does not affect our findings. The Ångström parameter, which is an integral indicator of size and relative concentration for the fine and coarse aerosol fractions, shows no trend. On the other hand, the SSA was found to increase by ~ 0.02 over 9 years at the 88% confidence level, which confirms the above MAIAC-AERONET analysis. To exclude effects of Beijing aerosol absorption seasonality [Eck et al., 2010] and uneven sampling, the SSA analysis was repeated with the winter months excluded. This removed most values below 0.85, but gave a similar result for the SSA increase (0.017), bringing it closer to the MAIAC assessment (~ 0.01). Finally, to understand the spatial extent of the effect, two sites in addition to Beijing were analyzed - XiangHe, located about 60km southeast of Beijing in the downwind direction, and Taihu (120.215°E, 31.421°N) located about 1000 km south of Beijing. Both sites have shorter time records, starting in summer 2005. As expected, results for XiangHe show an increase in SSA (~ 0.03) similar to nearby Beijing, whereas data from 2005 till June 2010 for the remote Taihu site show a very small negative trend.

3. Discussion

A few years prior to the Beijing Olympic Games, the Chinese government embarked on efforts to lower air pollution in the Olympic host cities, including Beijing and its five surrounding provinces, targeting primarily the significant pollution sources such as transportation, industrial, and coal-burning activities [e.g., Wang *et al.*, 2010]. As a result, over 50,000 coal-burning homes were converted to natural gas. A number of industrial polluters were either modernized, including 16,000 coal-burning factories, or shut down by 2008. Many factories were relocated from Beijing, including the 4th largest steel company (Shougang Group), whose production was cut by 73% in 2008, and was completely phased out in December 2010. After 2007, the diesel vehicle emission standard was raised from Euro III to Euro IV in Beijing and from Euro II to Euro III for the rest of the country. Although a reduction in total air pollution in Beijing since 2005 [Lin *et al.*, 2010] and during the 2008 Olympics [Cermak and Knutti, 2009] as a result of these measures has been reported, there are several mitigating factors: *a)* although emissions of regulated sources such as SO₂ and primary particulate matter (PM) from cement production, coal combustion, and biofuel burning, were reduced, emissions of other less-controlled aerosol precursors (e.g., nitrogen compounds) are estimated to have grown [Lin *et al.*, 2010]; *b)* GDP has increased over 9% annually since 2007 except in 2009 (~6%), and the number of vehicles in Beijing and throughout the country has grown by 49% for the period 2007-2010; *c)* the meteorology and regional aerosols in Beijing play an important role [Streets *et al.*, 2007], which complicates the analysis, as discussed below.

Regional contributions to the Beijing aerosol load vary depending on their origin: highly absorbing aerosol, due mainly to residential heating and cooking (SSA=0.8-0.85), is brought in from the rural North, whereas the heavily industrialized South-West and South brings low absorbing, secondary aerosols (SSA=0.9-0.95), whose absorption is further reduced by hygroscopic growth in moist air [Garland *et al.*, 2009; Eck *et al.*, 2010]. A particular aerosol realization is the superposition of

diurnal [Garland *et al.*, 2009], synoptic (~5-7 days) [Streets *et al.*, 2007; Jia *et al.*, 2008], and seasonal [Eck *et al.*, 2010] patterns. Synoptic variation is linked to the passage of cold fronts from the North, which produce a gradual rotation of wind direction from the North to the South-West/South, with a simultaneous reduction of wind speed, creating stagnant conditions. This periodic variation gives rise to a saw-tooth-like pattern of suspended PM [Jia *et al.*, 2008], which is superimposed on the local diurnal cycle. This behavior is modulated by the seasonal pattern, which is dominated by northern airmasses in winter and humid southern airmasses in summer. Source apportionment simulations [Matsui *et al.*, 2009] reveal that for Beijing, the primary aerosols, including BC, are controlled by emissions from within 100 km around the city over the preceding 24 h, whereas emissions from as far away as 500 km over the previous three days were found to affect secondary aerosols.

Although regional aerosols make it difficult to assess the total PM reduction, they have less effect on aerosol absorption and its change with time. Indeed, the local aerosols contain highly absorbing BC from primary sources. The regional (secondary) aerosol may contain as much as, or more of the total carbon, but its light-absorption efficiency is significantly reduced due to the chemical/physical modifications of hygroscopic growth and aging. Even though regulations reduced total carbon, the absorption properties of secondary aerosols could not change much. By contrast, the reduction of BC from local (primary) sources leads to a measurable reduction of total absorption, as detected and described in this article. Our finding is supported by the long-term measurements of PM chemical composition in Beijing [Okuda *et al.*, 2011], which reported an observed 33% BC reduction in 2008 as compared to the reference period of 2005-2007.

4. Conclusions

In this work, we demonstrated a measurable reduction of the aerosol absorption over Beijing during 2007-2010 compared to the previous five years, most probably caused by the regulation of BC emissions. Two independent methods based on the time series analysis of a) MODIS-AERONET AOT data, and b) AERONET SSA data, give similar results, which are in qualitative agreement with in situ chemical composition analysis [Okuda *et al.*, 2011]. The coarse assessment based on the MAIAC-AERONET AOT regression slopes indicates a reduction of the imaginary refractive index of about 0.001, corresponding to an increase in single scattering albedo by ~ 0.01 , close to the AERONET SSA-change assessment of ~ 0.02 . The timing of these changes is correlated with expansive measures adopted by the Chinese government to improve air quality in Beijing in the wake of the 2008 Olympic Games.

Acknowledgements. The research of A. Lyapustin, Y. Wang and S. Korkin was funded by the NASA Terrestrial Ecology Program (Dr. D. Wickland), NASA Applications Program (Dr. L. Friedl, B. Doorn) and in part by the NOAA GOES-R program (Dr. M. Goldberg). The first author thanks S. Platnick for a fruitful discussion on data analysis.

REFERENCES

- Cermak, J., and R. Knutti (2009), Beijing Olympics as an aerosol field experiment, *Geophys. Res. Lett.*, *36*, L10806, doi:10.1029/2009GL038572.
- Chen, W.-T., R. Kahn, D. Nelson, K. Yau, and J. Seinfeld (2008), Sensitivity of multi-angle imaging to optical and microphysical properties of biomass burning aerosols, *J. Geophys. Res.* *113*, D10203, doi:10.1029/2007JD009414.
- Dubovik, O. and M. D. King (2000), A flexible inversion algorithm for retrieval of aerosol optical properties from Sun and sky radiance measurements, *J. Geophys. Res.*, *105*, 20,673-20,696.

206 Dubovik, O., B. Holben, T. F. Eck. et al. (2002), Variability of absorption and optical properties of
 207 key aerosol types observed in worldwide locations, *J. Atmos. Sci.*, 59, 590-608.

208 Eck, T. F, B. N. Holben, A. Sinyuk et al. (2010), Climatological aspects of the optical properties of
 209 fine/coarse mode aerosol mixtures, *J. Geophys. Res.*, 115, D19205, doi:10.1029/2010JD014002.

210 Garland, R., et al. (2009), Aerosol optical properties observed during Campaign of Air Quality
 211 Research in Beijing 2006 (CAREBeijing-2006): Characteristic differences between the inflow
 212 and outflow of Beijing city air, *J. Geophys. Res.*, 114, D00G04, doi:10.1029/2008JD010780.

213 Guinot, B., H. Cachier, J. Sciare, Y. Tong, W. Xin, and Y. Jianhua (2007), Beijing aerosol:
 214 Atmospheric interactions and new trends, *J. Geophys. Res.*, 112, D14314,
 215 doi:10.1029/2006JD008195.

216 Holben, B. N., T. F. Eck, I. Slutsker et al. (1998), AERONET-A Federated Instrument Network and
 217 Data Archive for Aerosol Characterization, *Rem. Sens. Environ.*, 66, 1-16.

218 Holben, B. N., T. F. Eck, I. Slutsker et al. (2006), AERONET's Version 2.0 quality assurance
 219 criteria, *Proc. SPIE*, 6408, 64080Q, doi: 10.1117/12.706524.

220 Hsu, N.C, Tsay S. C., King, M. D., et al. (2004), Aerosol properties over bright-reflecting source
 221 regions, *IEEE Trans. Geosci. Remote Sensing*, 42, 557-569.

222 Ichoku, C. D., A. Chu, S. Mattoo et al. (2002), A spatial-temporal approach for global validation and
 223 analysis of MODIS aerosol products, *Geophys. Res. Lett.*, 29, doi: 10.1029/2001GL013206.

224 Intergovernmental Panel on Climate Change (2007), Climate Change 2007: The Physical Science
 225 Basis. Contribution of Working Group I to the Fourth Assessment Report of the
 226 Intergovernmental Panel on Climate Change, edited by S. Solomon et al., 996 pp., Cambridge
 227 Univ. Press, Cambridge, U. K.

228 Jia, Y., K. A. Rahn, K. He, T. Wen, Y. Wang (2008), A novel technique for quantifying the regional
 229 component of urban aerosol solely from its sawtooth cycles, *J. Geophys. Res.*, *113*, D21309,
 230 doi:10.1029/2008JD010389.

231 Kahn, R.A., B.J. Gaitley, M.J. Garay et al. (2010), MISR aerosol product assessment by comparison
 232 with AERONET, *J. Geophys. Res.*, *115*, D23209, doi: 10.1029/2010JD014601.

233 Lei, Y., Q. Zhang, K. B. He, D. G. Streets (2010), Primary aerosol emission trends for China, 1990–
 234 2005, *Atmos. Chem. Phys. Discuss.*, *10*, 17153–17212, doi:10.5194/acpd-10-17153-2010.

235 Levy, R. C., L. Remer, S. Mattoo, E. Vermote, and Y. J. Kaufman (2007), Second-generation
 236 algorithm for retrieving aerosol properties over land from MODIS spectral reflectance, *J.*
 237 *Geophys. Res.*, *112*, D13211, doi: 10.1029/2006JD007811.

238 Lin, J., C. Nielsen, Y. Zhao, Y. Lei, Y. Liu, M. McElroy (2010), Recent Changes in Particulate Air
 239 Pollution over China Observed from Space and the Ground: Effectiveness of Emission Control,
 240 *Environ. Sci. Technol.*, *44*, 7771–7776.

241 Lyapustin, A., et al., (2011), Multi-Angle Implementation of Atmospheric Correction (MAIAC):
 242 Part 2. Aerosol Algorithm, *J. Geophys. Res.*, *116*, D03211, doi:10.1029/2010JD014986.

243 Martonchik, J.V., R.A. Kahn, and D.J. Diner (2009), Retrieval of Aerosol Properties over Land
 244 Using MISR Observations, in *Satellite Aerosol Remote Sensing Over Land*, edited by
 245 Kokhanovsky, A.A. and G. de Leeuw, pp. 267-293 , Springer, Berlin.

246 Matsui, H. , M. Koike, Y. Kondo et al. (2009), Spatial and temporal variations of aerosols around
 247 Beijing in summer 2006: Model evaluation and source apportionment, *J. Geophys. Res.*, *114*,
 248 D00G13, doi:10.1029/2008JD010906.

- Meier, J., B. Wehner, A. Massling et al. (2009), Hygroscopic growth of urban aerosol particles in Beijing (China) during wintertime: a comparison of three experimental methods, *Atmos. Chem. Phys.*, *9*, 6865–6880, 2009.
- Okuda, T., Matsuura, S., Yamaguchi, D. et al. (2011), The impact of the pollution control measures for the 2008 Beijing Olympic Games on the chemical composition of aerosols, *Atmos. Environ.*, doi: 10.1016/j.atmosenv.2011.01.053 (in press).
- Ramana, M. V., V. Ramanathan, Y. Feng, S-C. Yoon, S-W. Kim, G. R. Carmichael and J. J. Schauer (2010), Warming influenced by the ratio of black carbon to sulphate and the black-carbon source, *Nature Geoscience*, *3*, 542-545, doi: 10.1038/NGEO918.
- Smirnov A., B. N. Holben, T. F. Eck, O. Dubovik, and I. Slutsker (2000), Cloud screening and quality control algorithms for the AERONET data base, *Rem. Sens. Environ.*, *73*, 337-349.
- Streets, D. G., et al. (2007), Air quality during the 2008 Beijing Olympic Games, *Atmos. Environ.*, *41*, 480 – 492, doi:10.1016/j.atmosenv.2006.08.046.
- Torres, O., Tanskanen, A., Veihelmann P., et al. (2007), Aerosols and surface UV products from Ozone Monitoring Instrument observations: An overview. *J. Geophys. Res.*, *112*, D24S47, doi:10.1029/2007JD008809.
- Wang, G., J. Bai, Q. Kong, and A. Emilenko (2005), Black carbon particles in the urban atmosphere in Beijing, *Adv. Atmos. Sci.*, *22*, 640– 646.
- Wang et al. (2010), Quantifying the Air Pollutants Emission Reduction during the 2008 Olympic Games in Beijing, *Environ. Sci. Technol.*, *44*, 2490-2496.

Figure 1. Time series showing MAIAC and AERONET AOT data over Beijing at $0.47\ \mu\text{m}$, for 10 years of MODIS Terra (top) and ~9 years of MODIS Aqua (bottom). The arrow indicates the approximate boundary between periods I and II.

Figure 2. Time series difference plots $(\text{AERONET} - \text{MAIAC AOT})_{0.47}$ for moderate-to-high atmospheric opacity ($\text{AERONET AOT} > 0.4$) over Beijing, showing MODIS Terra (left) and Aqua (right).

Figure 3. Time series plots of AERONET effective radius for fine aerosol fraction (left) and single scattering albedo (right) for the Beijing site. Points represent monthly averaged values.

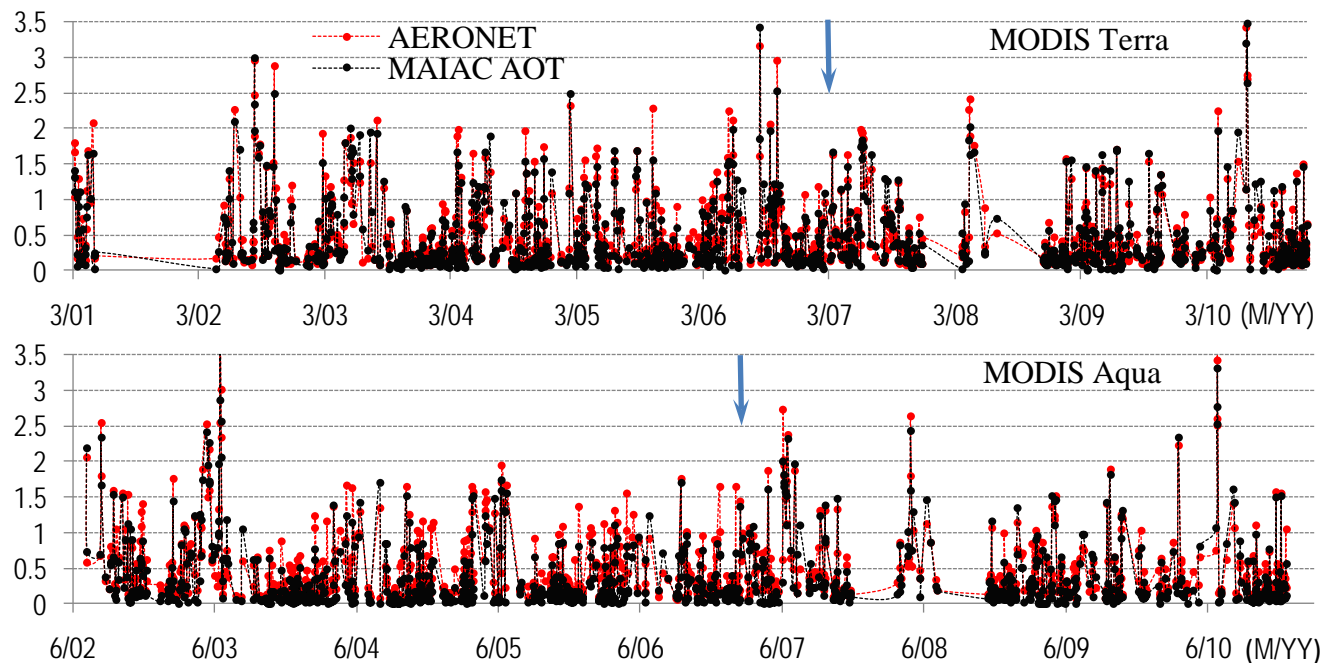


Figure 1. Time series showing MAIAC and AERONET AOT data over Beijing at $0.47 \mu\text{m}$, for 10 years of MODIS Terra (top) and ~9 years of MODIS Aqua (bottom). The arrow indicates the approximate boundary between periods I and II.

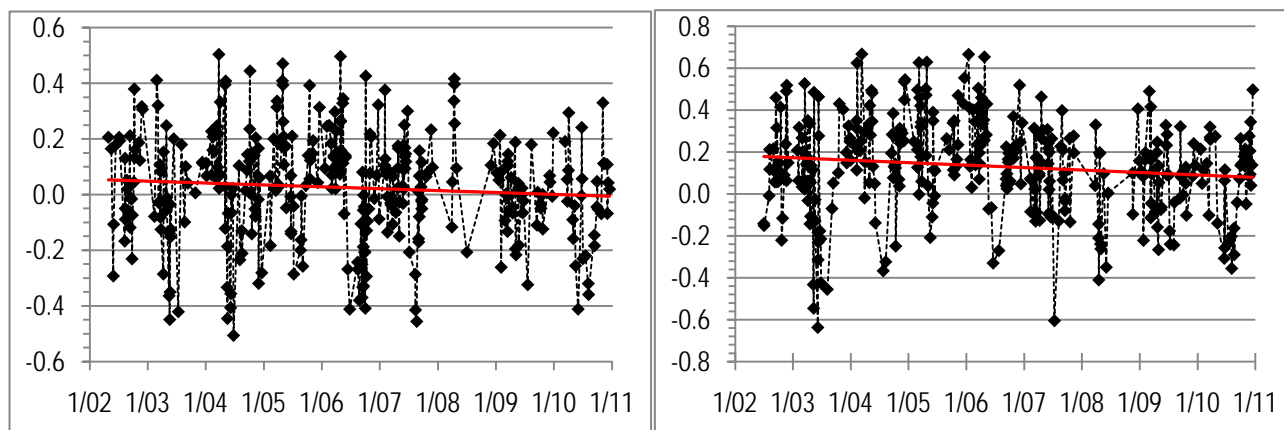


Figure 2. Time series difference plots $(\text{AERONET} - \text{MAIAC AOT})_{0.47}$ for moderate-to-high atmospheric opacity ($\text{AERONET AOT} > 0.4$) over Beijing, showing MODIS Terra (left) and Aqua (right).

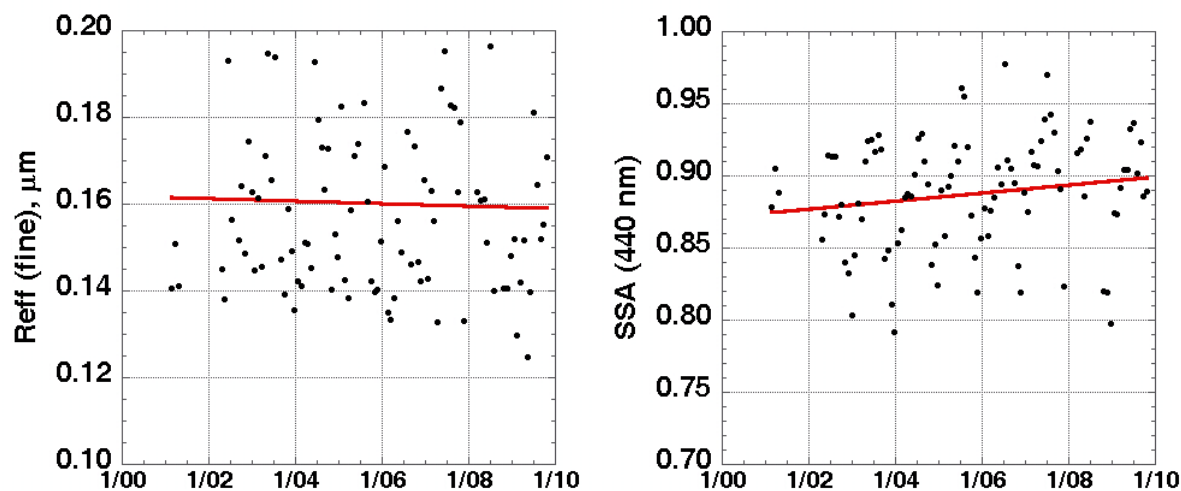


Figure 3. Time series plots of AERONET effective radius for fine aerosol fraction (left) and single scattering albedo (right) for the Beijing site. Points represent monthly averaged values.